

Active and Passive Beamforming Design for Reconfigurable Intelligent Surface Assisted CR-NOMA Networks

Wei Liang, *Member, IEEE*, Wei Luo, *Student Member, IEEE*, Jiankang Zhang, *Senior Member, IEEE*, Zhiguo Ding, *Fellow, IEEE*

Abstract—In this paper, a underlay cognitive radio inspired non-orthogonal multiple access (CR-NOMA) network assisted by the reconfigurable intelligent surface (RIS) technique is conceived to maximize the energy efficiency (EE), while all the cognitive users (CUs) are located in the “dead zone”. In particular, the CUs could only receive the information from the cognitive base station (CBS) via RIS. The EE maximization optimization problem which is a non-convex problem has been constructed to realize joint beamforming design at both the CBS and RIS with the constraints of the primary user’s (PU) interference power restriction and the CUs’ rate fairness. Moreover, we propose the alternating pragmatic iterative algorithm (APIA) to optimize the non-convex optimization problem until the final value of EE converges. Based on the simulation results, our proposed algorithm attains the significant gain than the two benchmarks of the random phase scheme as well as the fixed phase scheme on the RIS.

Index Terms—Reconfigurable Intelligent Surface, Cognitive Radio, Non-orthogonal Multiple Access, Energy Efficiency.

I. INTRODUCTION

In the sixth-generation (6G) wireless networks, the frequency range will migrate to higher frequency bands such as terahertz (THz) due to the resource shortage problem. Hence, it is imperative to develop disruptively new and innovative technologies in order to achieve a sustainable capacity growth with low and affordable overhead, complexity, as well as the energy consumption [1]. Non-orthogonal multiple access (NOMA) has been introduced as a promising radio access technology to efficiently improve utilization of spectrum resources for 6G wireless networks. The key idea of NOMA technique is to serve multiple users in the same spectrum, where superposition coding (SC) and successive interference cancellation (SIC) can be utilized at the transmitter and receiver respectively [2]. Moreover, underlay cognitive radio (CR) has been treated as another potential research direction of improving the spectrum efficiency and mitigating the shortage of spectrum for the future wireless networks. The key idea of underlay CR networks is that the cognitive users (CUs) are allowed to access the spectrum of the primary users (PUs) as long as the interference caused by CUs meets a certain demand [3]. In order to jointly exploit the benefits offered by the above two techniques, many researches have been conducted on underlay CR-NOMA networks.

In the future, the communication range will become smaller due to various attenuations. However, the underlay CR-NOMA networks cannot provide services when CUs are in the “dead zone” of the communication. To solve this intractable problem, reconfigurable intelligent surface (RIS) is introduced as a novel technique for the 6G wireless networks [4]. The surface contains a large number of

reconfigurable passive components, each of which can be used to control the phase and amplitude of the incident signal. Therefore, the RIS can provide supplementary communication links between the cognitive base station (CBS) and CUs when the line-of-sight (LoS) path is not available. Additionally, the existing works have been proved that the networks with RIS can improve the channel capacity and the system security [5], [6].

At present, there are several works focusing on the beamforming design with the RIS. But there are many distinctions compared with our works. The system model of [5] have not established in CR-NOMA networks and the optimization variable only involves the passive beamforming on the RIS after some simplifications. Thus, the process of optimization is different in comparison with ours. Then, due to the different optimization problem of [7], even if the similar conventions are used, there are many distinctions in the approximation process. Finally, the considered algorithm of [8] is completely different from ours, although our aims are to maximize energy efficiency.

In this letter, we consider a downlink underlay CR-NOMA network assisted by RIS which aims to maximize the energy efficiency (EE) while the CUs are located in the “dead zone” of the communication. In our conceived networks, we construct a non-convex optimization problem to realize joint beamforming design at both the CBS and RIS with the constraints of the PU’s interference power limit, the CUs’ rate fairness, and the users’ quality of service (QoS). Then, the alternative pragmatic iterative algorithm (APIA) is proposed to calculate both the active and passive beamforming. In the simulations, the proposed APIA algorithm is capable of improving the network’s energy efficiency and reducing the power consumptions.

II. SYSTEM MODEL

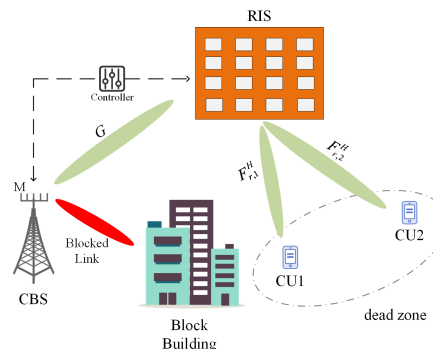


Fig. 1. System model of RIS assisted CR-NOMA networks.

In this paper, we consider a RIS-assisted underlay CR-NOMA network, which consists of a primary network, multiple single-antenna CUs $U_i, i = 1, 2$ and a M-antenna cognitive base station (CBS). Without loss of generality, two single-antenna CUs at the destination receive the information simultaneously by employing the NOMA technique. As shown in Fig. 1, both of the CUs are in the “dead zone” and they could not successfully receive the information from CBS due to building occlusion. However, the RIS is capable of reflecting the information from CBS to ensure that CUs could receive the information wherever they located. Without loss of generality, the CBS can perfectly estimate the channel state information (CSI)

The work was supported by the Shenzhen Science and Technology program under Grant JCYJ20210324121006017 and in part by the Foundation of State Key Laboratory of Integrated Services Networks of Xidian University under Grant ISN22-03, and in part by National Nature Science Foundation of China under Gants 62101450.

Wei Liang is with the Research & Development Institute of Northwestern Polytechnical University in Shenzhen, Shenzhen, 518057, China, and also with the State Key Laboratory of Integrated Services Networks, Xidian University, Xi’an, 710071, China. Wei Liang and Wei Luo are with the School of Electronics Information, Northwestern Polytechnical University, Xi’an, 710072, China. Jiankang Zhang is with the Department of Computing and Informatics, Bournemouth University, UK. Zhiguo Ding is with the school of Electrical and Electronic Engineering, University of Manchester, UK. Email: liangwei@nwpu.edu.cn; vinci@mail.nwpu.edu.cn; jzhang3@bournemouth.ac.uk; zhiguo.ding@manchester.ac.uk.

between CBS and CUs, and then the quasi-static flat-fading model is considered [9].

Let $\Theta = \text{diag}(\gamma) \in \mathbb{C}^{N \times N}$ as the diagonal reflection coefficients matrix of the RIS with $\gamma = [\gamma_1, \gamma_2, \dots, \gamma_N]$ and $\gamma_n = \beta_n e^{j\theta_n}$, where $\beta_n \in [0, 1]$ and $\theta_n \in [0, 2\pi)$ denote the amplitude and phase shift of the n th RIS element, respectively. In our conceived networks, the non-ideal RIS scheme is considered, that is, each element of RIS has a fixed amplitude, such as $\beta_n = 1$ [9].

The channel gain from CBS to RIS and from RIS to U_i are denoted by $\mathbf{G} \in \mathbb{C}^{N \times M}$ and $\mathbf{F}_{r,i}^H \in \mathbb{C}^{1 \times N}$, respectively, where \mathbf{F}^H denotes the conjugate transpose of \mathbf{F} . The channel gain from the RIS to PU and from primary base station (PBS) to RIS are denoted as $\mathbf{H}_{PI}^H \in \mathbb{C}^{1 \times N}$ and $\mathbf{H}_{BPI} \in \mathbb{C}^{N \times 1}$, respectively. In order to utilize the SIC technology in NOMA, the channel gain of the CUs should sort as $|\mathbf{F}_{r,1}^H \Theta \mathbf{G}|^2 \geq |\mathbf{F}_{r,2}^H \Theta \mathbf{G}|^2$, where $|\bullet|$ represents the modulus of a complex scalar. Therefore, the decoding order is $U_2 > U_1$.

Moreover, s_i and s_P denote the information-bearing symbol for the i th CU and the PU with zero mean and unit variance. The complex baseband signal transmitted from the CBS is given by $\mathbf{X} = \mathbf{w}_1 s_1 + \mathbf{w}_2 s_2$, where $\mathbf{w}_i \in \mathbb{C}^{M \times 1}$ is the active beamforming vector for the i th CU. Thus, the received signal at U_i can be expressed as

$$y_i = \mathbf{F}_{r,i}^H \Theta \mathbf{G} \mathbf{X} + \mathbf{F}_{r,i}^H \Theta \mathbf{H}_{BPI} \sqrt{P_P} s_P + n_i, \quad (1)$$

where the transmission power of the PBS is defined as P_P and $n_i \sim CN(0, \sigma^2)$ is the additive white Gaussian noise (AWGN) at user i with zero mean and variance σ^2 .

Thus, the interference power received by the PU can be expressed as

$$y_P = \mathbf{H}_{PI}^H \Theta \mathbf{G} (\mathbf{w}_1 s_1 + \mathbf{w}_2 s_2). \quad (2)$$

Then, the interference power constraint imposed on the PU should be constrained as [10]

$$\left| \mathbf{H}_{PI}^H \Theta \mathbf{G} \mathbf{w}_1 \right|^2 + \left| \mathbf{H}_{PI}^H \Theta \mathbf{G} \mathbf{w}_2 \right|^2 \leq P_{P,th}, \quad (3)$$

where $P_{P,th}$ is the maximum interference power at the PU's receiver.

Furthermore, the users rate fairness need to be fully considered in the NOMA group. Thus, the following constraints have been considered

$$\left| \mathbf{F}_{r,i}^H \Theta \mathbf{G} \mathbf{w}_2 \right|^2 \geq \left| \mathbf{F}_{r,i}^H \Theta \mathbf{G} \mathbf{w}_1 \right|^2, \quad i = 1, 2. \quad (4)$$

Based on the NOMA principle, the user with higher channel gain can use the SIC to eliminate the interference from other users. Therefore, the signal-interference-plus-noise ratio (SINR) to decode U_i 's information at the U_j 's receiver can be computed as

$$\phi_{j,i} = \frac{\left| \mathbf{F}_{r,j}^H \Theta \mathbf{G} \mathbf{w}_i \right|^2}{\left| \mathbf{F}_{r,j}^H \Theta \mathbf{G} \mathbf{w}_{i-1} \right|^2 + \left| \mathbf{F}_{r,j}^H \Theta \mathbf{H}_{BPI} \right|^2 P_P + \sigma^2}, \quad j \leq i, \quad (5)$$

where $\left| \mathbf{F}_{r,1}^H \Theta \mathbf{G} \mathbf{w}_0 \right|^2 = 0$. Then, the corresponding rate is expressed as $R_{j,i} = \log_2(1 + \phi_{j,i})$. In order to guarantee the achievable rates of the CUs are greater than their minimal rate requirement $R_{i,\min} = \log_2(1 + \phi_{i,\min})$, which are

$$R_i = \min(R_{j,i}) \geq R_{i,\min}, \quad j \leq i. \quad (6)$$

The $\min\{\bullet\}$ means the U_i 's achievable rate meets the minimize rate requirement at any receiver.

The goal of this paper is to maximize the networks' EE by jointly optimizing the active beamforming at the CBS and the passive beamforming on the RIS. The EE is defined as the ratio of the sum rate to the total power consumption. The total power consumption consists of two parts, one used to transmit signal and the other is the circuit consumption at the CBS. The power amplifier efficiency is defined as $\eta \in [0, 1]$. P_l is the total circuit consumption at the CBS.

P_{CBS} is the maximum transmission power of the CBS. Therefore, the energy efficiency optimization problem can be established as [11]

$$(P1) : \max_{(\mathbf{w}_1, \mathbf{w}_2, \Theta): \theta_n \in [0, 2\pi], \forall n} \frac{R_1 + R_2}{\frac{1}{\eta} \sum_{i=1}^2 \|\mathbf{w}_i\|^2 + P_l}, \quad (7)$$

$$s.t. \quad R_i \geq R_{i,\min}, \quad i = 1, 2, \quad (7a)$$

$$\sum_{i=1}^2 \|\mathbf{w}_i\|^2 \leq P_{CBS}, \quad (7b)$$

$$(3), (4), \quad (7c)$$

where $\|\bullet\|$ represents the Euclidean norm of a vector. Eq.(7a) guarantees the CUs' QoS. Eq.(7b) describes the maximum transmission power of the CBS. Eq.(3) guarantees the PU's QoS that the interference power caused by CUs do not exceed the tolerable limit. Eq.(4) ensures the CUs rate fairness within a NOMA group. However, the expression of R_i is not jointly convex with respect to $\{\mathbf{w}_i\}$ and Θ . Then, Eq.(7) is not the concave function. It is hard to obtain the global solution for this non-convex problem.

III. BEAMFORMING OPTIMIZATION SOLUTION

In this section, by decomposing the original problem into active beamforming optimization and passive beamforming optimization, APIA algorithm based on successive convex approximation (SCA) and semi-definite relaxation (SDR) is proposed in order to solve these two sub-optimization problems.

A. Active Beamforming Optimization

For the given passive beamforming on the RIS, the original problem can be converted into problem (P2) by introducing the slack variable α

$$(P2) : \max_{\mathbf{w}_1, \mathbf{w}_2, \alpha} \alpha \quad (8)$$

$$s.t. \quad \frac{R_1 + R_2}{\frac{1}{\eta} \sum_{i=1}^2 \|\mathbf{w}_i\|^2 + P_l} \geq \alpha, \quad (8a)$$

$$(7a), (7b), (7c). \quad (8b)$$

Without loss of generality, the non-convex constraint (8a) can equivalently be decomposed into the following two constraints by introducing another slack variable ν

$$R_1 + R_2 \geq \alpha \nu, \quad (9)$$

$$\nu \geq \frac{1}{\eta} \sum_{i=1}^2 \|\mathbf{w}_i\|^2 + P_l. \quad (10)$$

Obviously, Eq.(10) can be transferred into convex set by using second-order cone (SOC)

$$\left\| \begin{array}{c} \frac{\eta\nu - \eta P_l - 1}{2} \\ \mathbf{w}_1 \\ \mathbf{w}_2 \end{array} \right\| \leq \frac{1 - \eta P_l + \eta\nu}{2}. \quad (11)$$

Additionally, by introducing slack variable $\{\varphi_i\}$ to express the R_i , then Eq.(9) can be represented as follows

$$\sum_{i=1}^2 \log_2(\varphi_i) \geq \alpha \nu, \quad (12)$$

$$1 + \varphi_i \geq \varphi_i, \quad i = 1, 2, \quad (13)$$

where ϕ_i is the corresponding SINR of R_i . To eliminate the log function of Eq.(12), we introduce another slack variable $\{\gamma_i\}$, then

$$\sum_{i=1}^2 \gamma_i \geq \alpha \nu, \quad (14)$$

$$2^{\gamma_i} \leq \varphi_i, \quad i = 1, 2. \quad (15)$$

By using these slack variables, Eq.(9) can be equivalently transferred to Eq.(13), Eq.(14) and Eq.(15). Although Eq.(13) is linear, ϕ_i is non-convex with respect to the optimization variable \mathbf{w}_i . Therefore, further optimization is required in the following. Moreover, by calculating the Hessian matrix, we conclude that Eq.(15) is a convex function about γ_i and φ_i .

To handle the non-convex function of Eq.(13), slack variable $\{\rho_{j,i}\}$ is using to reformulate it, as shown in the following two expressions

$$\left| \mathbf{F}_{r,j}^H \Theta \mathbf{G} \mathbf{w}_i \right|^2 \geq (\varphi_i - 1) \rho_{j,i}, \quad (16)$$

$$\left| \mathbf{F}_{r,j}^H \Theta \mathbf{G} \mathbf{w}_{i-1} \right|^2 + \left| \mathbf{F}_{r,j}^H \Theta \mathbf{H}_{BPI} \right|^2 P_P + \sigma^2 \leq \rho_{j,i}, \quad j \leq i. \quad (17)$$

However, Eq.(17) can be proved that it is a convex set. By considering the arbitrary rotation to the phase of beamforming vector \mathbf{w}_i , then the imaginary part of $\mathbf{F}_{r,j}^H \Theta \mathbf{G} \mathbf{w}_i$ is zero. Thus, Eq.(16) can be converted into

$$\text{Re}(\mathbf{F}_{r,j}^H \Theta \mathbf{G} \mathbf{w}_i) \geq \sqrt{(\varphi_i - 1) \rho_{j,i}}, \quad (18)$$

$$\text{Im}(\mathbf{F}_{r,j}^H \Theta \mathbf{G} \mathbf{w}_i) = 0. \quad (19)$$

The right side of Eq.(18) can be approximated by the first-order Taylor series, then use SCA to transfer this non-convex constraint to convex expression. Thus, Eq.(18) can be equivalently transferred into

$$\begin{aligned} \text{Re}(\mathbf{F}_{r,j}^H \Theta \mathbf{G} \mathbf{w}_i) &\geq \sqrt{(\varphi_i^{(n)} - 1) \rho_{j,i}^{(n)}} + \frac{1}{2} \sqrt{\frac{\rho_{j,i}^{(n)}}{\varphi_i^{(n)} - 1}} \\ &\left(\varphi_i - \varphi_i^{(n)} \right) + \frac{1}{2} \sqrt{\frac{\varphi_i^{(n)} - 1}{\rho_{j,i}^{(n)}}} \left(\rho_{j,i} - \rho_{j,i}^{(n)} \right), \end{aligned} \quad (20)$$

where $\varphi_i^{(n)}$ and $\rho_{j,i}^{(n)}$ are the n th iteration values of φ_i and $\rho_{j,i}$, respectively. Similarly, Eq.(14) can be transferred as

$$\sum_{i=1}^2 \gamma_i \geq \alpha^{(n)} \nu^{(n)} + \nu^{(n)} \left(\alpha - \alpha^{(n)} \right) + \alpha^{(n)} \left(\nu - \nu^{(n)} \right), \quad (21)$$

where $\alpha^{(n)}$ and $\nu^{(n)}$ are the n th iteration values of α and ν . Therefore, for given the n th optimized values, the $(n+1)$ th optimized values can be obtained by using Eq.(20) and Eq.(21).

Then, similar to Eq.(11), Eq.(3) and Eq.(7a) can be transformed by SOC algorithm, which are given by the following expressions respectively

$$\left\| \begin{array}{l} \mathbf{H}_{PI}^H \Theta \mathbf{G} \mathbf{w}_1 \\ \mathbf{H}_{PI}^H \Theta \mathbf{G} \mathbf{w}_2 \end{array} \right\| \leq \sqrt{P_{P,th}}, \quad (22)$$

and

$$\left\| \begin{array}{l} \mathbf{F}_{r,j}^H \Theta \mathbf{G} \mathbf{w}_1 \\ \vdots \\ \mathbf{F}_{r,j}^H \Theta \mathbf{G} \mathbf{w}_{i-1} \\ \mathbf{F}_{r,j}^H \Theta \mathbf{H}_{BPI} \sqrt{P_P} \\ \sigma \end{array} \right\| \leq \frac{\text{Re}(\mathbf{F}_{r,j}^H \Theta \mathbf{G} \mathbf{w}_i)}{\sqrt{\phi_{i,\min}}}. \quad (23)$$

Additionally, due to Eq.(19), Eq.(4) can be equivalently converted into

$$\text{Re}(\mathbf{F}_{r,j}^H \Theta \mathbf{G} \mathbf{w}_2) \geq \text{Re}(\mathbf{F}_{r,j}^H \Theta \mathbf{G} \mathbf{w}_1), \quad j = 1, 2. \quad (24)$$

By incorporating all of these approximations, the optimization problem (P2) can be formulated into the following problem

$$(P3): \max_{\mathbf{w}_i, \alpha, \nu, \varphi, \gamma, \rho} \alpha \quad (25)$$

$$\text{s.t.} (7b), (11), (15), (17), (19) - (24). \quad (25a)$$

For the optimized variables initialization, we need to guarantee the feasibility and convergence in the process of optimization. Firstly find the suitable $\mathbf{w}_i^{(0)}$ by using Eq.(7a) Eq.(7b) and Eq.(7c). Then, $\rho_{j,i}^{(0)}$, $\varphi_i^{(0)}$, $\nu^{(0)}$ and $\alpha^{(0)}$ are found by Eq.(17), Eq.(16), Eq.(10) and Eq.(8a) respectively. Additionally, $\gamma_i^{(0)}$ and $EE^{(0)}$ can be computed by Eq.(14) and Eq.(7). In each iteration, we utilize the above all variables' value to get new variables' value, until the optimization problem satisfies the convergence criteria δ .

B. Passive Beamforming Optimization

In this section, we optimize the passive beamforming vector on the RIS by the given active beamformation vector $\{\mathbf{w}_i\}$. The original energy efficiency optimization problem (P1) can be transformed to

$$(P4): \max_{(\Theta): \theta_n \in [0, 2\pi], \forall n} R_1 + R_2 \quad (26)$$

$$\text{s.t.} (7a), (7c). \quad (26a)$$

For convenience of subsequent processing, let $\mathbf{F}_{r,j}^H \Theta \mathbf{G} \mathbf{w}_i = \boldsymbol{\mu}^H \mathbf{b}_{j,i}$, $\mathbf{H}_{PI}^H \Theta \mathbf{G} \mathbf{w}_i = \boldsymbol{\mu}^H \mathbf{c}_i$ and $\mathbf{F}_{r,j}^H \Theta \mathbf{H}_{BPI} = \boldsymbol{\mu}^H \mathbf{d}_j$, where $\boldsymbol{\mu}^H = [e^{j\theta_1}, \dots, e^{j\theta_N}]$, $\mathbf{b}_{j,i} = \text{diag}(\mathbf{F}_{r,j}^H) \mathbf{G} \mathbf{w}_i$, $\mathbf{c}_i = \text{diag}(\mathbf{H}_{PI}^H) \mathbf{G} \mathbf{w}_i$ and $\mathbf{d}_j = \text{diag}(\mathbf{F}_{r,j}^H) \mathbf{H}_{BPI}$. Then, due to the data transmission rate R_i is a $\min\{\bullet\}$ function, we introduce the slack variable ξ to transform the original problem into the following equations

$$(P5): \max_{(\xi, \Theta): \theta_n \in [0, 2\pi], \forall n} \xi \quad (27)$$

$$\text{s.t.} R_1 + R_{1,2} \geq \xi, \quad (27a)$$

$$R_1 + R_{2,2} \geq \xi, \quad (27b)$$

$$(7a), (7c). \quad (27c)$$

However, this is still a non-convex problem due to Eq.(27b). But if the lower bound of $R_1 + R_{2,2}$ can be found, the ξ could infinitely approach to its lower bound. According to the sort of channel gain, we can obtain $|\boldsymbol{\mu}^H \mathbf{b}_{1,1}|^2 \geq |\boldsymbol{\mu}^H \mathbf{b}_{2,1}|^2$. Expand the expression of $R_1 + R_{2,2}$ and let ξ approach its lower bound, then we obtain

$$\begin{aligned} R_1 + R_{2,2} &\geq \log_2 \left(\frac{|\boldsymbol{\mu}^H \mathbf{b}_{2,2}|^2 + |\boldsymbol{\mu}^H \mathbf{b}_{2,1}|^2 + |\boldsymbol{\mu}^H \mathbf{d}_2|^2 P_P + \sigma^2}{|\boldsymbol{\mu}^H \mathbf{d}_1|^2 P_P + \sigma^2} \right) \\ &\geq \xi. \end{aligned} \quad (28)$$

The $R_1 + R_{1,2}$ can be further simplified as the following

$$R_1 + R_{1,2} = \log_2 \left(1 + \frac{|\boldsymbol{\mu}^H \mathbf{b}_{1,1}|^2 + |\boldsymbol{\mu}^H \mathbf{b}_{1,2}|^2}{|\boldsymbol{\mu}^H \mathbf{d}_1|^2 P_P + \sigma^2} \right) \geq R_1 + R_{2,2}. \quad (29)$$

Thus, another slack variable $\Gamma = 2^\xi - 1$ can be used to eliminate the log function. After that the problem (P5) can be equivalently expressed as

$$(P6): \max_{\boldsymbol{\mu}, \Gamma} \Gamma \quad (30)$$

$$\text{s.t.} \frac{|\boldsymbol{\mu}^H \mathbf{b}_{2,2}|^2 + |\boldsymbol{\mu}^H \mathbf{b}_{2,1}|^2 + |\boldsymbol{\mu}^H \mathbf{d}_2|^2 P_P - |\boldsymbol{\mu}^H \mathbf{d}_1|^2 P_P}{|\boldsymbol{\mu}^H \mathbf{d}_1|^2 P_P + \sigma^2} \geq \Gamma, \quad (30a)$$

$$\frac{|\boldsymbol{\mu}^H \mathbf{b}_{1,1}|^2}{|\boldsymbol{\mu}^H \mathbf{d}_1|^2 P_P + \sigma^2} \geq \phi_{1,\min}, \quad (30b)$$

$$\frac{|\boldsymbol{\mu}^H \mathbf{b}_{j,2}|^2}{|\boldsymbol{\mu}^H \mathbf{b}_{j,1}|^2 + |\boldsymbol{\mu}^H \mathbf{d}_j|^2 P_P + \sigma^2} \geq \phi_{2,\min}, \quad j = 1, 2, \quad (30c)$$

$$|\boldsymbol{\mu}^H \mathbf{c}_1|^2 + |\boldsymbol{\mu}^H \mathbf{c}_2|^2 \leq P_{P,th}, \quad (30d)$$

$$|\boldsymbol{\mu}^H \mathbf{b}_{j,2}|^2 \geq |\boldsymbol{\mu}^H \mathbf{b}_{j,1}|^2, \quad j = 1, 2. \quad (30e)$$

Since variables in the right hand of Eq.(30a) can be expressed as $\Gamma \left(|\boldsymbol{\mu}^H \mathbf{d}_1|^2 P_P + \sigma^2 \right)$, it is the non-convex expression and SCA is applied to tackle this by introducing the slack variable κ which is similar to Eq.(20) and Eq.(21). Then, all the constraints can be transformed into quadratic constraints, then we apply SDR algorithm to approximately solve problem (P6). Let $\mathbf{U} = \boldsymbol{\mu} \boldsymbol{\mu}^H$, $\mathbf{B}_{j,i} = \mathbf{b}_{j,i} \mathbf{b}_{j,i}^H$,

$C_i = c_i c_i^H$ and $D_j = d_j d_j^H$. Additionally, U should satisfy $U \succeq 0$ and $\text{Rank}(U) = 1$. Albeit the constraint of rank 1 is a non-convex constraint. By applying SDR, the problem (P6) can be rewritten as

$$(P7) : \max_{U, \Gamma} \Gamma \quad (31)$$

$$s.t. \quad \text{Tr}(UD_1) P_P + \sigma^2 \leq \kappa, \quad (31a)$$

$$\begin{aligned} & \text{Tr}(UB_{2,2}) + \text{Tr}(UB_{2,1}) + \text{Tr}(UD_2) P_P \\ & - \text{Tr}(UD_1) P_P \geq f(\Gamma^{(n)}, \kappa^{(n)}), \end{aligned} \quad (31b)$$

$$\frac{\text{Tr}(UB_{1,1})}{\text{Tr}(UD_1) P_P + \sigma^2} \geq \phi_{1,\min}, \quad (31c)$$

$$\frac{\text{Tr}(UB_{j,2})}{\text{Tr}(UB_{j,1}) + \text{Tr}(UD_j) P_P + \sigma^2} \geq \phi_{2,\min}, \quad j = 1, 2, \quad (31d)$$

$$\text{Tr}(UC_1) + \text{Tr}(UC_2) \leq P_{P,th}, \quad (31e)$$

$$\text{Tr}(UB_{j,2}) \geq \text{Tr}(UB_{j,1}), \quad j = 1, 2, \quad (31f)$$

$$U_{kk} = 1, \quad k = 1, \dots, N, \quad (31g)$$

$$U \succeq 0, \quad (31h)$$

where $f(\Gamma^{(n)}, \kappa^{(n)}) = \Gamma^{(n)} \kappa^{(n)} + \Gamma^{(n)} (\kappa - \kappa^{(n)}) + \kappa^{(n)} (\Gamma - \Gamma^{(n)})$ at the given feasible point $(\Gamma^{(n)}, \kappa^{(n)})$ and $\text{Tr}(x)$ is the trace of x . U is a positive semidefinite matrix and the diagonal elements become 1. Additionally, problem (P7) is an instance of semidefinite programming (SDP). Then we could use CVX program to solve problem (P7). After obtaining the optimized variable U^* 's value, the singular value decomposition (SVD) or Gaussian randomization method can be applied to get μ^* .

C. Complexity and Convergence of APIA

In the above analysis, we decompose the original problem (P1) into two optimization subproblems which are (P3) and (P7). The details of APIA algorithm are summarized in Algorithm 1. In this section, we explain the complexity and convergence of our proposed algorithm.

For the problem (P3), we convert it into second-order cone programming (SOCP) form, and use SCA algorithm to calculate iteratively. The number of decision variables n is in the order of $2M+10$. Therefore, the total complexity based on the SCA algorithm is given by [12]

$$\mathcal{O}\left(nL_1\sqrt{30}(12n + (2M+2)^2 + 112 + n^2) \ln(1/\epsilon)\right), \quad (32)$$

where L_1 is the number of iterations and ϵ denotes the computation accuracy.

For the problem (P7), it consists of $N+8$ linear constraints and one linear matrix inequality (LMI) constraint with the size of N . The number of decision variables n is on the order of N^2+1 . Therefore the total complexity can be expressed as

$$\begin{aligned} & \mathcal{O}\left(nL_2\sqrt{2N+8}\right. \\ & \left.(nN^2 + 8n + nN + 8 + N + N^3 + n^2) \ln(1/\epsilon)\right), \end{aligned} \quad (33)$$

where L_2 is the number of iterations.

Combining the above two parts, we can obtain the total complexity of APIA algorithm which is

$$\begin{aligned} & \mathcal{O}\left(I_{ite}^N \left(nL_1\sqrt{30}(12n + (2M+2)^2 + 112 + n^2) \ln(1/\epsilon) + nL_2 \right. \right. \\ & \left. \left. \sqrt{2N+8}(nN^2 + 8n + nN + 8 + N + N^3 + n^2) \ln(1/\epsilon) \right) \right), \end{aligned} \quad (34)$$

where I_{ite}^N denotes the number of iterations for APIA algorithm.

Let $EE(w^l, \mu^l)$, $EE_w(w^l, \mu^l)$ and $EE_\mu(w^l, \mu^l)$ be the optimization problems (P1), (P3) and (P7) respectively at the l th iteration,

then we have [9]

$$\begin{aligned} EE(w_i^l, \mu^l) & \stackrel{(a)}{=} EE_w(w_i^l, \mu^l) \stackrel{(b)}{\leq} EE_w(w_i^{l+1}, \mu^l) \\ & \stackrel{(c)}{\leq} EE(w_i^{l+1}, \mu^l) \stackrel{(d)}{\leq} EE_\mu(w_i^{l+1}, \mu^{l+1}) \\ & \stackrel{(e)}{\leq} EE(w_i^{l+1}, \mu^{l+1}). \end{aligned} \quad (35)$$

Step (a) means the first-order Taylor series for given local point are compact in optimization problem (P3). Step (b) holds since the optimization problem (P3) is solved by $\{w_i^{l+1}\}$. Step (c) illustrates the optimization problem (P3) as the lower bound of optimization problem (P2). Then, step (d) and step (e) are similar to step (b) and step (c). Although the optimization variables involve three matrices, Eq.(35) indicates that the optimization problem (P1) calculated by APIA algorithm is non-decreasing after each iteration. Meanwhile, the value of EE cannot increase indefinitely due to the constraints of the maximum CBS's transmission power and the interference power restriction at PU's receiver. Therefore, the proposed algorithm is guaranteed to be convergent.

Algorithm 1: APIA algorithm for obtaining beamforming

- 1 **Initialization:** the passive beamforming $\mu^{(0)}$ on the RIS and the outer iteration, $i = 1$.
 - 2 Set $\{w^{(0)}, \alpha^{(0)}, \nu^{(0)}, \varphi^{(0)}, \gamma^{(0)}, \rho^{(0)}, EE^{(0)}\}$ and the inner iteration, $j = 1$.
 - 3 **repeat;**
 - 4 Solve Problem (P3) by using the given $\mu^{(i)}$, where the optimal solution is denoted by $\{w_j^*, \alpha_j^*, \nu_j^*, \varphi_j^*, \gamma_j^*, \rho_j^*\}$.
 - 5 **if** $|\alpha_j^* - \alpha^{(j-1)}| \leq \delta$
 - 6 Output: α_j^* and w_j^* ,
 - 7 **else**
 - 8 Set $\{w^{(j)}, \alpha^{(j)}, \nu^{(j)}, \varphi^{(j)}, \gamma^{(j)}, \rho^{(j)}\} = \{w_j^*, \alpha_j^*, \nu_j^*, \varphi_j^*, \gamma_j^*, \rho_j^*\}$ and let $j = j + 1$ then return to step 3.
 - 9 **end if**
 - 10 Set $\{\Gamma^{(0)}, \kappa^{(0)}\}$, $l = 1$ and solve problem (P7) by using the given w_j^* , where the optimal solution is denoted by U^* until $|\Gamma^{(l)} - \Gamma^{(l-1)}| \leq \delta$.
 - 11 Utilize the SVD or the Gaussian randomization method to obtain μ^* .
 - 12 Calculate $EE^{(i)}$ by μ^* and w_j^* .
 - 13 **if** $|EE^{(i)} - EE^{(i-1)}| \leq \delta$
 - 14 Output: $EE^* = EE^{(i)}$,
 - 15 **else**
 - 16 Let $i = i + 1$ and return to step 2.
 - 17 **end if**
-

IV. SIMULATIONS RESULTS AND ANALYSIS

In this section, the simulation results are obtained to illustrate the effectiveness of our proposed algorithm. The CBS and RIS are equipped with a uniform linear array (ULA) and uniform rectangular array (URA) respectively. Then all the channel conditions are assumed as Rician fading model [5]. The path loss exponents of CBS-RIS and RIS-CU are set as 3.2 and 2 respectively. In our simulations, one of the CUs is located near the CBS, and the other is located at the edge of the cell. So the distance between RIS and CUs are about 10m and 28m respectively, then, the distance between RIS and CBS is 10m. Furthermore, let us set up: 1) the noise power is $\sigma^2 = -60dBm$, 2) the transmit power of the CBS and PBS are $P_{CBS} = 20dBm$ and $P_P = 40dBm$, 3) the power amplifier efficiency is $\eta = 0.7$, 4) the maximum interference power is at the PU's receiver $P_{P,th} = -70dB$, 5) the convergence criteria $\delta=0.01$.

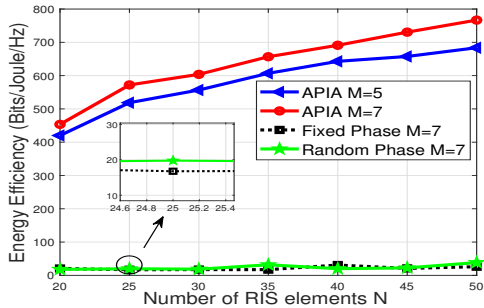


Fig. 2. EE versus number of RIS elements N .

Fig. 2 illustrates the relationship between the number of RIS elements and system's EE under the different antenna numbers at the CBS. We set the total circuit power at the CBS, $P_l = 10dBm$. Additionally, the random phase scheme and the fixed phase scheme refer to the EE calculated by optimizing active beamforming with the random and fixed passive beamforming. The fixed passive beamforming means $\theta_n = \pi$, $n = 1, \dots, N$. By increasing the number of RIS elements, the system's EE of proposed algorithm is increasing. However, for the other two schemes, the corresponding EE is hardly increased. So that, these two schemes do not achieve the best match between active beamforming and passive beamforming in the process of optimization. Then the destructive interference occurs after reflection by the RIS, which leads to a decreasing total rate. Subsequently, it can be found that increasing the number of CBS antennas achieves a performance gain of the system's EE.

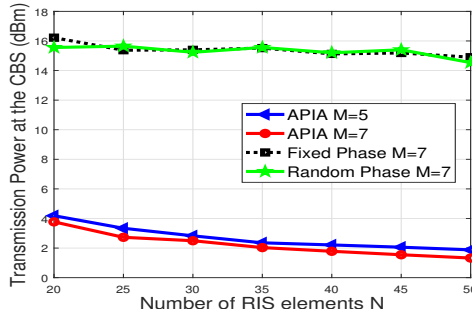


Fig. 3. Transmission power versus number of RIS elements N .

In Fig. 3, the relationship between the number of RIS elements and the transmission power at the CBS for different schemes is dedicated. In particular, the simulation parameters are consistent with Fig. 2. Fig. 3 shows that the APIA scheme requires lower power to obtain the maximum EE at the CBS than other schemes under any number of RIS elements. Furthermore, it is interesting to note that no matter how large the number of RIS elements is, the CBS's transmission power is almost constant based on the random phase scheme and the fixed phase scheme. Only optimize the active beamforming, which leads to the waste of energy. Therefore, we conclude that the proposed algorithm obtains a higher system's EE and power consumption performance compared with other two benchmarks.

As shown in Fig. 4, the relationship between the circuit power at the CBS and the system's EE by using different schemes, while the CBS antenna sets $M = 3$. As the number of RIS elements increases, the EE also increases. Simultaneously, when the circuit power at the CBS is small, the optimized beamforming brings greater changes to the EE. Therefore, as P_l increases, the slope of energy efficiency becomes decreasing. From this, we can obtain that when the value of the circuit power is low, the system's beamforming is dominant in the EE. Additionally, the proposed algorithm can achieve higher system's EE under different circuit power. We conclude that the system with the proposed algorithm always outperforms the system with the random phase scheme and the fixed phase scheme.

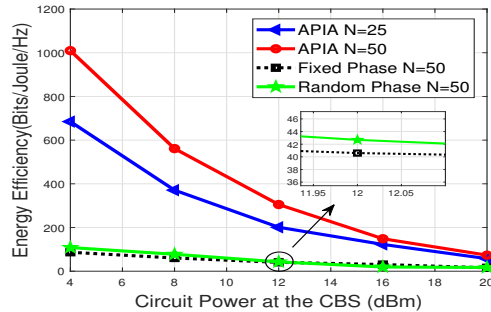


Fig. 4. EE versus circuit power P_l at the CBS.

V. CONCLUSIONS

In this paper, a CR-NOMA network assisted by RIS has been developed aiming to maximize the system's energy efficiency. To achieve maximum energy efficiency, the original problem can be decomposed into two subproblems, which are active beamforming optimization problem and passive beamforming optimization problem. In particular, the APIA algorithm is proposed to optimize both the active and passive beamforming. Based on the simulation results, our proposed algorithm achieves a higher energy efficiency compared with the fixed phase scheme and random phase scheme. As for transmission power, the proposed algorithm could require lower power at the CBS compared with these two benchmarks. Additionally, the system performance is improved as the number of antenna at the CBS or RIS elements increase.

REFERENCES

- [1] Q. Wu, S. Zhang, B. Zheng, C. You, and R. Zhang, "Intelligent Reflecting Surface-Aided Wireless Communications: A Tutorial," *IEEE Trans. Commun.*, vol. 69, no. 5, pp. 3313–3351, May 2021.
- [2] W. Wang, X. Liu, J. Tang, N. Zhao, Y. Chen, Z. Ding, and X. Wang, "Beamforming and Jamming Optimization for IRS-Aided Secure NOMA Networks," *IEEE Trans. Wirel. Commun.*, vol. 21, no. 3, pp. 1557–1569, Mar 2022.
- [3] A. V. and Babu A. V., "Performance Analysis of NOMA-Based Underlay Cognitive Radio Networks With Partial Relay Selection," *IEEE Trans. Veh. Technol.*, vol. 70, no. 5, pp. 4615–4630, May 2021.
- [4] C. Huang, S. Hu, G. C. Alexandropoulos, A. Zappone, C. Yuen, R. Zhang, M. D. Renzo, and M. Debbah, "Holographic MIMO Surfaces for 6G Wireless Networks: Opportunities, Challenges, and Trends," *IEEE Wirel. Commun.*, vol. 27, no. 5, pp. 118–125, Oct 2020.
- [5] Q. Wu and R. Zhang, "Intelligent Reflecting Surface Enhanced Wireless Network via Joint Active and Passive Beamforming," *IEEE Trans. Wirel. Commun.*, vol. 18, no. 11, pp. 5394–5409, Nov 2019.
- [6] F. Fang, Y. Xu, Q.-V. Pham, and Z. Ding, "Energy-Efficient Design of IRS-NOMA Networks," *IEEE Trans. Veh. Technol.*, vol. 69, no. 11, pp. 14088–14092, Nov 2020.
- [7] C. Pan, H. Ren, K. Wang, M. Elkashlan, A. Nallanathan, J. Wang, and L. Hanzo, "Intelligent Reflecting Surface Aided MIMO Broadcasting for Simultaneous Wireless Information and Power Transfer," *IEEE J. Sel. Areas Commun.*, vol. 38, no. 8, pp. 1719–1734, Aug 2020.
- [8] C. Huang, A. Zappone, G. C. Alexandropoulos, M. Debbah, and C. Yuen, "Reconfigurable Intelligent Surfaces for Energy Efficiency in Wireless Communication," *IEEE Trans. Wirel. Commun.*, vol. 18, no. 8, pp. 4157–4170, Aug 2019.
- [9] X. Mu, Y. Liu, L. Guo, J. Lin, and N. Al-Dhahir, "Exploiting Intelligent Reflecting Surfaces in NOMA Networks: Joint Beamforming Optimization," *IEEE Trans. Wirel. Commun.*, vol. 19, no. 10, pp. 6884–6898, Oct 2020.
- [10] J. Yuan, Y.-C. Liang, J. Joung, G. Feng, and E. G. Larsson, "Intelligent Reflecting Surface-Assisted Cognitive Radio System," *IEEE Trans. Commun.*, vol. 69, no. 1, pp. 675–687, Jan 2021.
- [11] A. Zappone, M. Di Renzo, F. Shams, X. Qian, and M. Debbah, "Overhead-Aware Design of Reconfigurable Intelligent Surfaces in Smart Radio Environments," *IEEE Trans. Wirel. Commun.*, vol. 20, no. 1, pp. 126–141, Jan 2021.
- [12] X. Zhou, J. Li, F. Shu, Q. Wu, Y. Wu, W. Chen, and L. Hanzo, "Secure SWIPT for Directional Modulation-Aided AF Relaying Networks," *IEEE J. Sel. Areas Commun.*, vol. 37, no. 2, pp. 253–268, Feb 2019.